Modelling the effects of riparian vegetation on spray drift and dust: The role of local protection

Michael. R. Raupach, John F. Leys, Nicholas Woods, Gary Dorr and Helen A. Cleugh

Technical Report 29/00, August 2000

Modelling the effects of riparian vegetation on spray drift and dust: The role of local protection

M.R. Raupach[1], J.F. Leys[2], N. Woods[3], G. Dorr[3] and H.A. Cleugh[1]

[1]CSIRO Land and Water, GPO Box 1666, Canberra, ACT 2601, Australia
[2]Department of Land and Water Conservation, PO Box 462, Gunnedah, NSW 2380, Australia
[3]Centre for Pesticide Application and Safety, Gatton College, University of Queensland

Report to the NSW Department of Land and Water Conservation on Project PAT3

17 August 2000

Summary

The objective of this study is to develop scientifically based guidelines for the optimum ways that vegetation can be maintained or planted in the landscape to provide local protection for sensitive areas against spray or dust deposition.

Local protection occurs when particles (such as spray droplets or dust) are filtered out of the air flowing through a porous vegetative barrier such as a windbreak or narrow buffer strip. It can provide a high degree of protection against particle deposition for sensitive receptor surfaces (such as rivers or human habitation) close to the barrier. Local protection may be contrasted with regional protection, the enhanced removal of particles from the atmosphere at large scales by widespread tall vegetation over an extensive region.

The following guidelines are expressed in terms of properties of a vegetative barrier or windbreak which can be easily assessed by eye in the field: its height H and its optical porosity t_b. The latter can be estimated as the fractional visibility through the windbreak, from a viewpoint directly facing the windbreak.

Entrapment of particles by the windbreak: A theory for the entrapment of particles in the windbreak itself has been developed and tested against field data. This leads to the following simple guidelines:

- For particles of moderate size (30 μm) and larger, and for windbreaks with leaves less than around 30 mm wide, the fraction of particles transmitted through a windbreak is about the same as the optical porosity t_b, and the fraction entrapped by filtration of the airflow is about $(1-t_b)$. For small particles, or for windbreaks with very large leaves, a larger fraction than t_b is transmitted and a smaller fraction than $(1-t_b)$ is entrapped.

- The total number or mass of particles deposited to the windbreak is determined by a trade-off: the windbreak must be dense enough to absorb particles efficiently, but sparse enough to allow some particles to flow through and be trapped. The value of the optical porosity for maximum total deposition is typically around $t_b = 0.2$.

Attenuation of particle deposition to the surface in the lee of the windbreak: From a simple theory for the attenuation of particle deposition to the surface by local protection in the lee of the windbreak, the following guidelines emerge:

- The protection offered by a windbreak against particle deposition to the downwind surface arises from two effects: entrapment of particles by the windbreak, and wind shelter in the lee of the windbreak.

- Particle entrapment attenuates the deposition immediately behind the windbreak by a factor approximately equal to the optical porosity t_b, as above.

- Wind shelter attenuates the deposition in the immediate lee of the windbreak by about a factor t_b for small particles (around 10 μm and smaller). There is practically no effect of wind shelter on deposition for large particles (over 300 μm).

- Combining both effects, the reduction in deposition in the immediate lee of the windbreak due to both particle entrapment and wind shelter is a factor of about t_b^2 for moderate-sized (30 μm) particles and about t_b for large particles (over 300 μm). For instance, if the optical porosity is 25% = 0.25, then the deposition immediately behind the windbreak is reduced for small particles to about 0.25x0.25 = 0.06 of its upwind value, while for large particles it is reduced to about 0.25 of its upwind value.

- This protection is significant (deposition reduction relative to upwind of over 50%) for a shelter distance of 3 to over 10 windbreak heights downwind. Values at the lower end of this range are appropriate for rough upwind terrain, and at the higher end for smooth terrain. The protection then attenuates gradually with further distance downwind until it disappears at many tens of windbreak heights.

1 Introduction

One of the corporate goals of the DLWC is “to improve the health and productivity of the ecosystems of NSW”. A threat to health and productivity of ecosystems is the airborne contamination of rivers and landscapes (principally pastures) by spray droplets and dust, which cause off-site movement of agricultural chemicals. A means of reducing this contamination is through the use of shrubs and trees to suppress particle movement and thereby protect sensitive areas. Either existing native vegetation or strategically planted windbreaks or buffer strips can be employed. To maximise the effectiveness of vegetation in providing protection against airborne spray and dust contamination, it is necessary to know how the deposition of particles to sensitive areas is influenced by the type and configuration of vegetation. From this knowledge, guidelines can be developed in a form suitable for use by vegetation management officers and committees currently working to implement the Native Vegetation Conservation Act 1997.

Vegetation provides protection against particle deposition in two different ways, acting respectively at regional scales (kilometres) and local scales (tens of metres). *Regional protection* occurs when particles are extracted from the air flowing *over* an extensive "buffer" area with a high potential for absorbing particles; *local protection* occurs when particles are filtered out of the air flowing *through* a porous vegetative barrier such as a windbreak. In general, regional protection can provide low to moderate shelter from particle deposition over extensive areas, while local protection provides a high degree of shelter over a small area.

This project is the third of a series of investigations funded by the NSW Department of Land and Water Conservation into airborne contamination of riverine and other environments by spray and dust movement, and the role of vegetation in providing protection against such contamination. These three studies are:

- PAT1: "Aerial Pathways Study: nutrient deposition to riverine environments", aimed at assessing the significance of nutrient deposition to riverine areas;
- PAT2: 'Modelling the effects of riparian vegetation on spray drift and dust" (Raupach and Leys 1999), formulating guidelines for regional protection; and

- PAT3: Modelling the effects of riparian vegetation on spray drift and dust: the role of local protection", the present study, formulating guidelines for local protection.

In this project (PAT3), local or short-range protection is examined by investigating two related effects that occur when spray or dust particles are filtered from an airflow by a porous vegetative barrier or windbreak: (1) the entrapment of particles on the barrier itself, and (2) the reduction in downwind deposition of particles to the ground, caused both by lower wind speeds and reduced particle concentrations in the lee of the vegetation. The specific objective is to quantify the ways that both entrapment within the vegetation and the reduced downwind deposition depend on the height, areal extent, density and leaf characteristics of the vegetation.

The project employs several techniques, drawing from the diverse areas of expertise of the five authors of this report:

- Theoretical modelling of wind flows around vegetation and the deposition of particles from the air to vegetated surfaces (mainly the responsibility of MRR);

- Analysis of field experiments on the deposition of particles to windbreaks, carried out from 1990 to 1992 by the Centre for Pesticide Application and Safety, Gatton College, University of Queensland, by NW, GD and colleagues;

- Wind tunnel investigations of the bulk aerodynamic properties of vegetative barriers, by HAC, MRR and colleagues;

- Synthesis of information from the above sources, mainly by JFL and MRR.

This report is organised into six sections: (1) the present introduction, (2) a short discussion of regional and local protection, (3) theoretical development, (4) wind tunnel experiments, (5) field experiments and (6) discussion and conclusions, including a statement of achievement of the deliverables specified in the Contract Agreement for Project PAT3. The report is also the basis of a scientific paper (Raupach *et al.* 2001).

2 Regional and Local Influences of Vegetation on Particle Deposition

The processes by which vegetation provides protection against particle deposition further downwind can be idealised in two different ways, acting respectively at regional and local scales (although the processes overlap to some extent). The following description is drawn from Raupach and Leys (1999).

Regional protection occurs when particles are extracted from the air flowing over an extensive "buffer" area with a high potential for absorbing particles, such as a wide vegetative buffer strip. The mechanism for this type of protection is as follows (Figure 1):

1. A relatively deep layer of particle-laden air, tens to hundreds of metres deep, is assumed to be produced by a particle source some distance upwind. The further upwind the source, the deeper is this layer. This incident flow is represented by point A.

2. The particle-laden air encounters a highly absorbing buffer surface, typically consisting of relatively tall vegetation with fine leaves. Particles are mixed downwards and deposited to this buffer surface, reducing particle concentrations in a "scrubbed" air layer which deepens with increasing distance (x) across the buffer surface; see point B.

3. Beyond the buffer surface, deposition to the downwind receptor surface is reduced. This occurs both because of the low particle concentrations in the scrubbed air layer itself (a relatively short-range effect), and also because particle concentrations in the entire particle-bearing layer are reduced by mixing and dilution of the remaining particle-laden air with the relatively clean air in the scrubbed layer (a long-range effect).

Local protection occurs when particles are filtered out of the air flowing through a porous vegetative barrier such as a windbreak or narrow buffer strip. The barrier, of height H, is assumed to be long in the cross-wind (y) direction and narrow in the along-wind (x) direction, and to be located at $x = 0$. The mechanism is as follows (Figure 2):

1. As in the regional case, the porous barrier is assumed to be immersed in a particle-laden air flow much deeper than the height H of the barrier itself, so that the incident particle concentration is approximately uniform with height; see point A.

2. Some of the oncoming air is filtered through the barrier while some passes over it. Particle concentrations are not changed in the air flowing over the barrier, but are strongly reduced in the through-flowing "bleed flow" by absorption onto leaves and stems in the barrier; see point B. There is a strong reduction in particle deposition to the surface in the immediate lee of the barrier, caused both by the reduced particle concentration and the reduced wind speed in this region, which corresponds with the "quiet zone" in the lee of the barrier. This region extends to a distance x of around $3H$ to $10H$ from the barrier. There is also a large deposition of particles to the barrier itself.

3. Particles in the flow above the barrier are mixed downwards into the quiet zone with increasing distance (x) from the barrier. Hence, near-surface particle concentrations and surface deposition both increase, eventually recovering approximately to their values upwind of the barrier. The local protection provided by a single barrier therefore effectively reduces deposition in the immediate lee of the barrier, but does not have much impact on concentrations further downwind.

In summary, regional protection occurs by downward deposition from the air flowing ***over*** an extensive buffer area, while local protection occurs by deposition or filtering as air flows ***through*** a single porous barrier. The distinction between the two mechanisms is not absolute, because repeated porous barriers (each providing local protection in its immediate lee) can constitute a buffer area which provides regional protection by scrubbing and diluting the particle-laden flow above. However, the distinction is useful because different modelling approaches are appropriate for the two cases. This focus of this report is on local protection, following the treatment of regional protection in Raupach and Leys (1999).

3 Theoretical Development

A significant amount of new or extended theory has been developed in the course of this work, described fully in Raupach *et al*. (2001). The theory involves five sequential steps, which in turn determine: (1) deposition of particles to a single vegetation element such as a leaf; (2) filtration of particles by an array of elements (such as a windbreak) from a flow of known velocity; (3) the velocity of the flow through the windbreak (the "bleed flow"); (4) the overall

deposition to the windbreak; and (5) the particle deposition to the downwind surface. These are outlined in the following five subsections, numbering the ideas within each subsection so that their development can be traced.

3.1 Deposition to a Single Vegetation Element

1. The deposition of particles to a single vegetation element occurs by two processes acting in parallel: inertial impaction of particles, and Brownian or quasi-molecular diffusion of particles through the boundary layer of the element (Slinn 1982, Davidson and Wu 1990).

2. The area-integrated particle flux or deposition rate D_e to a single element can be quantified by a conductance g_P such that $D_e = A_e g_P C$, where D_e is the deposition rate ($\mathrm{kg\,s^{-1}}$), C is the particle concentration in the flow to which the element is exposed ($\mathrm{kg\,m^{-3}}$), and A_e is the frontal surface area or silhouette area of the element ($\mathrm{m^2}$). Thus, g_P is a transfer coefficient with the dimension of velocity ($\mathrm{m\,s^{-1}}$). Considering separate conductances g_{Pi} and g_{Pb} for impaction and Brownian diffusion, we can write

$$D_e = A_e g_P C = A_e g_{Pi} C + A_t g_{Pb} C \qquad (1)$$

where A_t is the total surface area of the element (in contrast with the frontal area A_e).

3. The *impaction conductance* (g_{Pi}) can be related to the impaction efficiency E defined by the relationship $D_e = A_e EUC$, where U is the velocity to which the element is exposed. It follows that $g_{Pi} = EU$. The impaction efficiency is a function of wind speed, element size, particle size and particle-to-air density ratio, approaching 1 for large, heavy particles, small vegetation elements and high wind speeds. The expression used here to determine E is the same as used in Raupach and Leys (1999) and Raupach *et al*. (2000a,b). The *Brownian-diffusion conductance* (g_{Pb}) is determined by the diffusive transfer of a scalar through the laminar boundary layer around the vegetation element, which can be quantified by standard theory for the diffusive transfer of mass or heat (Raupach *et al*. 2000b).

4. Putting together the theoretical expressions for g_{Pi} and g_{Pb}, the overall conductance g_P (expressed as a fraction of the wind speed U around the vegetation element) is found to be

$$\frac{g_P}{U} = E + \left(\frac{A_1}{A_2}\right) C_{Pol}\ \mathrm{Re}^{-1/2}\ \mathrm{Sc}^{-2/3} \qquad (2)$$

where in the second term, C_{Pol} is the Polhausen coefficient (about 1.2 for a cylindrical element), Re is the Reynolds number for flow around the element, and Sc is the Schmidt number for Brownian particle diffusion (Monteith 1973, Finnigan and Raupach 1987). The term E on the right hand side is the impaction contribution and the second term is the contribution from Brownian diffusion. For particles of diameter greater than around 1 μm, impaction completely dominates Brownian diffusion (Raupach *et al.* 2000b), so it is possible to ignore the second term in Equation (2) and write $g_P/U \approx E$.

3.2 Filtration of Particles by a Windbreak

1. In this subsection we quantify the filtration of particles by a flow through a windbreak which is assumed to have known velocity U (the determination of this flow is done in the next subsection). Consider an airflow with an initial or upwind particle concentration C_0 (assumed independent of height), passing through a windbreak of streamwise length or thickness X_b. Air parcels travel through the windbreak along meandering trajectories because of the turbulence in the airflow, losing particles by deposition to windbreak elements as they move. If the frontal area density of the windbreak elements (the frontal area of elements per unit volume) is a_b, then the sink strength per unit volume for particles due to deposition is $a_b g_P C$ (kg m^{-3} s^{-1}).

2. Assuming that U, a_b and g_P can be regarded as constant along a trajectory, it follows that the fraction of particles remaining in the airflow after passage through the windbreak is

$$\frac{C_1}{C_0} = \exp\left(-\frac{g_P a_b S_b}{U}\right) \qquad (3)$$

where C_1 is the particle concentration in the flow emerging from the downwind side of the windbreak, and S_b is the total distance travelled by the air parcel in its trajectory through the windbreak. Because of the meandering of the turbulent flow through the windbreak, S_b is greater than the windbreak thickness X_b. We assume that $S_b/X_b = m$, where the "meander factor" m is the ratio of the total length of a trajectory (from $x = 0$ to X_b) to X_b itself. Clearly, m is somewhat

greater than 1. We take m = 1.2, from typical values of the turbulence intensity in flow through vegetation (Raupach *et al.* 1996).

3. Equation (3) can be cast in a more useful form by introducing the optical porosity of the windbreak, t_b. This is related to a_b and X_b by

$$t_b = \exp\left(-a_b X_b\right) \tag{4}$$

assuming that the transmission of light through the windbreak is governed by Beer's law. Most field observations of windbreak densities are given in terms of the easily measurable property t_b, rather than a_b and X_b. Hence, it makes sense to recast Equation (3) as

$$\frac{C_1}{C_0} = t_b \wedge \left[\left(S_b / X_b\right)\left(g_P / U\right)\right] = t_b \wedge \left[m\, g_P / U\right] \tag{5}$$

where ^ denotes the exponentiation operator ($x^a = x \wedge a$).

4. If Brownian diffusion is negligible relative to impaction, then g_P/U can be approximated by the impaction efficiency E and Equation (5) reduces to the simple form

$$\frac{C_1}{C_0} \approx t_b \wedge \left[mE\right] \tag{6}$$

5. An even simpler expression can be obtained as follows: for sufficiently large particles (in practice larger than around 30 μm), and for small vegetation elements (such as the needle-like leaves of Casuarinas or pines), E is close to (though less than) 1. Also, m is a little larger than 1. Hence we can assume $mE \approx 1$, so that

$$\frac{C_1}{C_0} \approx t_b \tag{7}$$

Hence, the fraction of large particles (exceeding around 30 μm) transmitted through a windbreak with small (needle-like) leaves is about the same as the optical porosity.

6. Figure 3 shows the particle transmission fraction C_1/C_0 predicted by full theory including both impaction and Brownian conductances, from Equation (5), plotted against the optical porosity t_b for several particle sizes d_p ranging from 10 to 160 μm (upper panel) and for several vegetation element sizes d_e ranging from 0.5 to 128 mm. Other assumed conditions are specified in the figure caption. For particle sizes d_p larger than around 30 μm and for d_e in the range 1 to 30 mm (that is, for all typical vegetation element sizes except very large), the very simple approximation $C_1/C_0 = t_b$ (Equation (7)) works well. For smaller particles, $C_1/C_0 > t_b$ because $E < 1$, so these small particles are less efficiently filtered from the airflow by the windbreak.

7. We also account for the fact that vegetation elements tend to streamline in a strong wind, so that the optical porosity t_b increases with increasing wind speed. We assume that a vegetation element behaves like a rigid stick suspended at the top, which hangs vertically in zero wind and has an equilibrium position at progressively greater angles from the vertical as wind speed increases. By calculating the balance of the turning moments due to gravity and drag, it can be shown that the angle of the stick in a uniform wind of speed U is

$$\tan\theta = \frac{2}{\pi}\frac{\rho_a}{\rho_e}\frac{c_d U^2}{g d_e} \qquad (8)$$

where ρ_a/ρ_e is the ratio of air density to the density of the element (stick), d_e is the diameter of the element, g is the gravitational acceleration and c_d is the drag coefficient of the element. The optical porosity of a windbreak in a wind (where elements are streamlining) is then related to the porosity t_{b0} in zero wind (where the elements hang vertically) by

$$t_b(U) = t_{b0}\cos\theta = t_{b0}\left(\frac{1}{1+\tan^2\theta}\right)^{1/2} \qquad (9)$$

This modifies t_b in Equations (5) to (7) to account for the streamlining of elements in a wind.

3.3 Windbreak Flow and Drag

1. It is necessary to determine the wind velocity U to which the elements are exposed. This is the velocity of the flow through the windbreak itself, or "bleed flow". Despite the wealth of

studies available on the influence of windbreaks on airflow, determination of the bleed velocity proves to be surprisingly difficult, because almost all studies are concerned with flows away from the windbreak and there are very few measurements of the flow through the windbreak itself. Accordingly, the determination of the bleed velocity has been a major focus of attention in this project. Our approach is to evaluate the bulk drag on the windbreak, firstly in terms of the bleed velocity and then from empirical knowledge of the drag forces on surface-mounted obstacles. Equating these two expressions yields an estimate for the bleed velocity.

2. The windbreak is treated as a relatively thin porous screen. When air flows through such a screen, the drag force per unit area of screen can be written as $\rho_a k U^2/2$, where k is a semi-empirical coefficient called the pressure coefficient (akin to a drag coefficient). In terms of the pressure coefficient and the bleed velocity, the drag on a windbreak is given by

$$F_b = \int_0^H \frac{\rho_a k U^2(0,z)}{2}\, dz \qquad (10)$$

where F_b is the total drag per unit cross-wind distance (Newton m^{-1}), H is the height of the windbreak, and $U(x,z)$ is the wind velocity at the point (x,z) (with x being the along-wind coordinate relative to the windbreak at $x = 0$, and z the height above the ground at $z = 0$). The bleed velocity as a function of height is therefore $U(0,z)$. We also define an average, height-independent bleed velocity U_b, such that

$$U_b = \left(\frac{1}{H} \int_0^H U^2(0,z)\, dz \right)^{1/2} \qquad (11)$$

Then, provided that the pressure coefficient k is uniform with height, Equation (10) becomes

$$F_b = \frac{\rho_a k U_b^2 H}{2} \qquad (12)$$

Henceforth, k is assumed to be uniform with height, so that Equation (12) holds. In other words, attention is restricted to windbreaks in which the density of the vegetation is approximately uniform with height, without significant gaps or trunk spaces.

3. The drag force F_b can also be expressed in terms of a reference wind velocity well away from the windbreak, say the wind velocity U_H at the windbreak height $z = H$, but at a value of x far enough upwind for the influence of the windbreak on the wind field $U(x,z)$ to be negligible. Such an expression uses the bulk windbreak drag coefficient Γ_b, defined by

$$\Gamma_b = \frac{F_b}{(r_a/2)U_H^2 H} \tag{13}$$

4. Equating the two expressions for the drag F_b, it is found that

$$U_b = U_H \left(\frac{\Gamma_b}{k} \right)^{1/2} \tag{14}$$

Hence, the relationship between the bleed velocity U_b and the reference velocity U_H can be found from the relationship between the bulk drag coefficient Γ_b and the pressure coefficient k of the "screen" of which the windbreak is made.

5. The relationship $\Gamma_b(k)$ can be determined semi-empirically by considering the limits of very porous and very dense windbreaks, as follows.

- For a very porous windbreak, the flow $U(0,z)$ through the windbreak is negligibly different from the reference flow $U(x_R,z)$ at a large distance x_R upwind of the windbreak, because the windbreak hardly perturbs the incident wind flow. Therefore, $U(0,z)$ in Equation (11) can be replaced by $U(x_R,z)$. For the present purpose, this upstream velocity profile can be approximated by a power-law profile $U(x_R,z) = U_H(z/H)^a$. The exponent a ranges from typically 1/7 over smooth (short grass) surfaces to typically 1/4 to 1/3 over rough (crop, shrub) surfaces. The integral in Equation (11) can then be evaluated explicitly, leading to

$$\Gamma_b = \frac{k}{k_1} \quad \text{or} \quad U_b^2 = \frac{U_H^2}{k_1} \quad \text{with} \quad k_1 = 1 + 2a \tag{15}$$

  so Γ_b is proportional to k.

- At the other extreme of a very dense windbreak, Γ_b is the same as the bulk drag coefficient for a solid fence, say Γ_{b1}, and is therefore independent of k. The bulk drag coefficient Γ_{b1} for a solid fence, defined by Equation (13), is known to be around 1.

It remains to construct a form for the function $\Gamma_b(k)$ which approaches k/k_1 as $k \to 0$ and approaches Γ_{b1} as $k \to \infty$. Though there are many possible functional forms which satisfy these limits, a convenient and simple form (to be tested experimentally) is

$$\Gamma_b = \frac{\Gamma_{b1} k}{k + \Gamma_{b1} k_1} \tag{16}$$

The coefficients Γ_{b1} and k_1 can be regarded as empirical, but there is a prior expectation that Γ_{b1} is not far from 1 and k_1 is in the range 1.3 to 1.6 (since $k_1 = 1+2a$, with a in the range 1/7 to 1/3, depending on surface roughness).

6. Combining Equations (14) and (16), the bleed velocity U_b is found to be

$$\frac{U_b}{U_H} = \left(\frac{\Gamma_{b1}}{k + \Gamma_{b1} k_1} \right)^{1/2} \tag{17}$$

This determines U_b as a function of the reference wind velocity U_H, for a windbreak with pressure coefficient k uniform with height. Tests of Equation (16) and (17) are presented later.

7. To complete this subsection, it is necessary to evaluate the pressure coefficient k for a windbreak. There are many theoretical and empirical formulae for k for porous materials such as gauzes, meshes and perforated plates. However, examination of the basis for these formulae shows that they are not appropriate for vegetative barriers, in essence because all formulae (even those for sparse screens) invoke the idea that the flow is constricted and therefore undergoes a pressure drop as it passes through the orifices in the screen. Such constriction does not occur for vegetative barriers to any significant extent. Instead, we use the idea that the total drag force per unit frontal area of the windbreak can be expressed in two ways: first as $r_a k U^2/2$ in terms of k (by its definition) and also as $r_a c_e a_b X_b U^2/2$, where c_e is the in-situ drag coefficient of a single windbreak element, a_b the frontal area density and X_b the windbreak thickness along the wind

direction (from the sum of the drag forces on windbreak elements). Equating these expressions and using Equation (4) to relate $a_b X_b$ to the optical porosity t_b, it is found that

$$k = c_e a_b X_b = -c_e \ln t_b \tag{18}$$

Figure 4 illustrates the relationship between k and t_b implied by Equation (18), comparing it with common equivalent expressions for porous screens. It is seen that the screen formulae predict substantially greater k for the same t_b. Equation (18) is more appropriate for windbreaks.

3.4 Particle Deposition to a Windbreak

1. The total particle deposition to the windbreak per unit crosswind length (kg m^{-1} s^{-1}) is

$$D_b = \int_0^H U(0,z)(C_0 - C_1)\, dz \tag{19}$$

2. Approximating $U(0,z)$ with U_b and $C_0 - C_1$ with Equation (6), we obtain

$$D_b \approx U_b H C_0 \left[1 - t_b \wedge (mE)\right] \tag{20}$$

3. The bleed velocity U_b is given in terms of t_b by Equations (17) and (18), so the final result for the total deposition D_b to a windbreak of optical porosity t_b is given by

$$D_b = U_H H C_0 \left(\frac{\Gamma_{b1}}{-c_e \ln t_b + \Gamma_{b1} k_1} \right)^{1/2} \left[1 - t_b \wedge (mE)\right] \tag{21}$$

4. This can be conveniently expressed as a bulk particle deposition coefficient Δ_b, a dimensionless number obtained by normalising D_b with the independent or externally specified parameters H (windbreak height), U_H (reference wind velocity) and C_0 (incident particle concentration). It follows that

$$\Delta_b = \frac{D_b}{U_H H C_0} = \left(\frac{\Gamma_{b1}}{-c_e \ln t_b + \Gamma_{b1} k_1} \right)^{1/2} \left[1 - t_b \wedge (mE)\right] \tag{22}$$

5. Equation (22) can be interpreted thus: the deposition to the windbreak is the product of two terms, one determining the bleed velocity and the other the fraction of particles entrapped by the windbreak (1 minus the fraction transmitted). Both terms are functions of the optical porosity t_b, but in opposite ways: the bleed velocity U_b increases from 0 as t_b increases from 0 to 1, whereas the fraction of particles entrapped $(1 - C_1/C_0)$ decreases from 1 to 0, roughly as $1-t_b$ according to Equation (7). Hence, the product of both terms is zero at both $t_b = 0$ and $t_b = 1$, and has a maximum at some intermediate value of t_b. Physically this occurs because particle deposition to a windbreak involves a trade-off: the windbreak must be dense enough to absorb particles efficiently, but sparse enough to allow some particles to flow through the windbreak and be filtered by it. If the windbreak is too dense then not enough particles can flow through it, the limit being a solid wall for which practically all particles are carried over the top of the barrier.

6. Figure 5 shows the prediction of Equation (22) for the bulk particle deposition coefficient as a plot of Δ_b against t_b (for conditions specified in the figure caption). The maximum in Δ_b is shown clearly, appearing at around $t_b = 0.2$ for large particles (at which point $\Delta_b \approx 0.45$) and at smaller t_b for smaller particles.

3.5 Particle Deposition to the Downwind Surface

1. The particle deposition to the ground surface (including the surface sheltered by the windbreak) can be written as

$$D_s = W_d C_r \tag{23}$$

where D_s is the deposition ($\mathrm{kg\,m^{-2}\,s^{-1}}$), C_r is the particle concentration ($\mathrm{kg\,m^{-3}}$) at a reference height just above the surface, and W_d is the deposition velocity ($\mathrm{m\,s^{-1}}$), a transfer coefficient or conductance describing the transfer of particles from the reference height to the surface (at which particles are assumed to be completely absorbed so that the concentration is zero).

2. The protection offered by a windbreak against particle deposition arises from two effects: (a) entrapment of particles by the windbreak, which reduces C_r in Equation (23), and (b) wind shelter in the lee of the windbreak, which reduces W_d. Figure 2 shows schematically how the

concentration C_r near the surface changes with distance downwind of the windbreak. The variation in the near-surface velocity is qualitatively similar (Judd *et al.* 1996).

3. The result of these effects can be quantified by writing the variation of the surface deposition D_s with streamwise distance x in the lee of the windbreak as

$$\frac{D_s(x)}{D_{s0}} = \frac{W_d(x)}{W_{d0}} \frac{C_r(x)}{C_0} \tag{24}$$

where upwind conditions (well away from the windbreak) are denoted by a subscript 0. The factors $W_d(x)/W_{d0}$ and $C_r(x)/C_0$ respectively describe the attenuation in the relative deposition $D_s(x)/D_{s0}$ through wind speed reduction and through concentration reduction by entrapment in the windbreak.

4. An idea of the behaviour of $C_r(x)/C_0$ can be obtained from simple, well-established theory in which the transport of a scalar entity through the air is described by a diffusion equation

$$U\frac{\partial C}{\partial x} = \frac{\partial^2 C}{\partial z^2} \tag{25}$$

Here the scalar is particles, with concentration $C(x,z)$. The wind velocity U and eddy diffusivity K are both assumed (crudely) to be constant. To determine $C(x,z)$ in the lee, the initial condition (defining the concentration profile immediately behind the windbreak at $x = 0$) is

$$C(0,z) = \begin{cases} C_1 & \text{for } 0 \le z \le H \\ C_0 & \text{for } z > H \end{cases} \tag{26}$$

The lower boundary condition at the ground ($z = 0$) is taken to be that the flux of C is zero (ignoring the small flux due to particle deposition). The solution of Equation (25) is then

$$C(x,z) = C_0 - \left(\frac{C_0 - C_1}{2}\right)\left[\text{erf}\left(\frac{H+z}{\sqrt{2}\,s_z(x)}\right) + \text{erf}\left(\frac{H-z}{\sqrt{2}\,s_z(x)}\right)\right] \tag{27}$$

where $\sigma_Z(x) = (2Kx/U)^{1/2}$ is the depth of the plume from a point source of scalar at a distance x downwind of the source. In particular, taking a reference height much less than the windbreak height H, we have

$$\frac{C_r(x)}{C_0} = \frac{C(x,0)}{C_0} = 1 - \left(1 - \frac{C_1}{C_0}\right)\mathrm{erf}\left(\frac{H}{\sqrt{2}\,\sigma_Z(x)}\right) \qquad (28)$$

5. The eddy diffusivity K can be approximated for the present purpose as the diffusivity in the upstream flow at windbreak height, so that:

$$K = k_{VK} u_* H\,, \qquad \sigma_Z(x) = \sqrt{2k_{VK}\frac{u_*}{U}\frac{x}{H}} \qquad (29)$$

where $k_{VK} = 0.4$ is the von Karman constant and u_* is the friction velocity. The ratio u_*/U depends on the roughness of the terrain around the windbreak, ranging from less than 0.1 in very smooth terrain (such as a windbreak on smooth bare ground) to more than 0.2 in very rough terrain (such as a windbreak surrounded by tall crops or orchards).

6. The downwind length X_s of the scalar sheltered region (in which $C_r(x)$ is substantially less than C_0) can be estimated as the distance at which $\sigma_Z(X_s) = H$. From Equation (29), this is given by $X_s/H = U/(2k_{VK}u_*) = 1.25U/u_*$. Hence, shelter length (normalised by the windbreak height) is in the range 3 to more than 10, being smaller for rougher terrain. This estimate accords with data on the shelter length, and its terrain dependence, for the wind field (Judd *et al.* 1996).

7. Figure 6 shows the behaviour of $C_r(x)/C_0$ from Equations (28) and (29), for three classes of upwind terrain: fairly smooth ($u_*/U = 0.1$), rough ($u_*/U = 0.2$) and very rough ($u_*/U = 0.3$). In all cases, C_1/C_0 was taken to be 0.1. There is a general trend for $C_r(x)/C_0$ to increase from C_1/C_0 just behind the windbreak, towards 1 at large distances downwind. The recovery towards 1 proceeds more slowly in smoother terrain.

8. We turn now to the role of reduced velocities in the lee of the windbreak, that is, the effect of W_d in Equation (24). The deposition velocity W_d is the sum of contributions from impaction and Brownian diffusion (as for particle entrapment by the windbreak) together with a contribution from gravitational particle settling:

$$W_d = W_t + G_{imp} + G_{brow} \quad (30)$$

where W_t is the terminal settling velocity of the particles, G_{imp} the bulk conductance to the surface due to impaction, and G_{brow} the bulk conductance due to Brownian diffusion. Raupach *et al.* (2000b) presented a model for W_d based on separate evaluation of each of these three terms. Figure 7a compares this model with data on particle-deposition to grass-like surfaces (Chamberlain 1967), indicating that the model gives satisfactory agreement with measurements. Figure 7b shows the contributions of the three terms W_t, G_{imp} and G_{brow} to W_d over the particle size range 0.01 to 1000 μm, showing that Brownian diffusion dominates for very small particles less than 0.1 μm, impaction dominates around 10 μm and settling for large particles of 100 μm or greater. Several inferences follow for the present purpose:

- Brownian diffusion (G_{brow}) is negligible, as for particle entrapment by a windbreak;
- Since W_t is independent of wind speed and G_{imp} is proportional to wind speed, the attenuation of the particle deposition by velocity reduction in the lee of a windbreak depends on particle size. For large particles (around 300 μm and larger), W_d is dominated by settling (W_t) and therefore the reduced velocity in the lee has no effect on W_d. For small particles (around 10 μm and smaller), W_d is dominated by impaction (G_{imp}) and so is proportional to the reduced velocity in the lee. For particles of intermediate size, the wind speed dependence of W_d, and hence the role of velocity reduction in limiting deposition, is between these extremes.
- A rough estimate of the maximum near-surface velocity reduction in the lee of the windbreak is that the lowest velocity (normalised by the upstream velocity at the same height) is around t_b, the optical porosity. Hence the minimum value of $W_d(x)/W_{d0}$ for small particles, just behind the windbreak, is around t_b, while for large particles $W_d(x)/W_{d0}$ is close to 1.

9. A summary of the implications of these findings is deferred to Section 6 (Conclusions).

4 Wind Tunnel Experiments on Windbreak Drag and Bleed Velocity

4.1 Aims and Methods

Wind tunnel measurements of the flow around model windbreaks have been used to test Equation (16) for the bulk drag coefficient Γ_b of a windbreak as a function of the pressure coefficient k, and to determine the coefficients Γ_{b1} and k_1. Two separate experiments were carried out in the Pye Laboratory wind tunnel, CSIRO Land and Water, Canberra. These are respectively described in detail by Judd *et al.* (1996, henceforth JRF) and Judd *et al.* (2000, henceforth JCH). In each experiment, model windbreaks of three densities were constructed from metal gauze and placed in a deep boundary layer flow set up to represent a thermally neutral atmospheric surface layer. The same three windbreak densities were used in both experiments. Velocity profiles were measured both upwind and downwind of the windbreaks with a triple-probe hot-wire anemometer.

The data used here are the velocity profiles measured immediately behind the windbreak, at $x/H = 0.1$. These were used to approximate the bleed flow through the windbreak itself, which could not be directly measured; in other words, we assumed that $U(0.1H, z) \approx U(0, z)$. The pressure coefficients (k) of the screens used to construct the windbreaks were also measured independently by placing a cross-section of each screen in a pipe and measuring the pressure drop across it at a sequence of known velocities through the pipe. From these measurements, the drag F_b on each windbreak was calculated using Equation (10), and the bulk windbreak drag coefficient Γ_b determined with Equation (13).

4.2 Results

Figure 8 shows the measurements of Γ_b plotted against k, together with the fit to the data from Equation (16). This equation describes the data quite successfully, with the empirical coefficients taking the values $\Gamma_{b1} = 0.75$, $k_1 = 1.5$. These are very reasonable values in view of the expectations stated following Equation (16). It is concluded that Equation (16) works well. This provides support for the use of Equation (17) to estimate for the bleed velocity U_b.

5 Field Measurements of Particle Entrapment by Windbreaks

5.1 Aims and Methods

Field measurements of the particle transmission fraction through a windbreak have been used to test the overall theory. The experiments were carried out from 1990 to 1992 by the Centre for Pesticide Application and Safety, Gatton College, University of Queensland, under the direction of the third and fourth authors of this report (NW, GD).

A total of 26 runs (three preliminary runs 1A to 1C and 23 experimental runs 1 to 23) were conducted on eleven different dates between 7 March 1990 and 15 October 1992, using five different windbreak configurations at three different sites (see Table 1):

- Windbreak 1: single-row Casuarina windbreak of height 9.5 m at the University of Queensland, Gatton College, Horticultural Field Section (Runs 1A to 1C);
- Windbreak 2: As for Windbreak 1, but a year later and with height 11 m (Runs 1 to 17);
- Windbreak 3: single-row Casuarina windbreak of height 11 m at the Alstonville Research Station, NSW (Runs 18 and 19);
- Windbreak 4: a two-row slash pine windbreak of height 9 m, on private property owned by Mr. Starcevich, via Alstonville, NSW (Runs 20 and 21);
- Windbreak 5: a four-row slash pine windbreak of height 7 m on the same property as Windbreak 4 (runs 22 and 23).

Each run involved a single-swathe release of spray well upwind of the windbreak (tractor-operated up to Run 17, hand-held for Runs 18 to 23). The spray particle size distribution was roughly log-normal with a median around 80 μm and a standard deviation of 0.25 for the tractor-operated releases, and with a slightly higher median for the hand-held releases. Tests were conducted in a variety of wind speeds, choosing conditions in which the mean wind direction was not too far from perpendicular to the windbreak.

The spray concentrations immediately upwind and downwind of the windbreaks were measured by two methods: (1) a fluorometric recovery technique, giving a measure of the droplet concentration (mass of droplets per unit volume of air); and (2) by counting droplet deposits (droplets/cm^2) on oil sensitive paper. Spray was recovered by using artificial targets. For fluorometry these were aluminium cylinders (50 mm long and 12.5 mm diameter). For the droplet-counting method the targets were sections of oil sensitive paper (52 x 39 mm) rolled into a cylindrical shape with an average diameter of 10 mm; droplet numbers per unit area were determined after cutting each cylinder along the long axis and gluing it to an A4 sheet of stiff cardboard, using image analysis (Optomax V) on 6 to 10 sample areas for each target.

Sampling was conducted using two telescopic towers supported with guy ropes. These were erected on the upwind and downwind side of the windbreak, to suspend the artificial targets. A piece of aluminium tubing with a T-piece at one end was placed on each tower to extend its height and allow two lines of artificial targets to be placed on the tower. The upwind tower for all tests was 14 m tall and placed approximately 2 m upwind of the windbreak. Sampling commenced at 1 m above the ground and continued at 1 m intervals to 14 m. The downwind tower was placed approximately one tree height behind the array. For some tests, sampling on the downwind tower was extended to a height of 18 m.

5.2 Results

Figures 9 to 12 show, for all windbreaks, the concentration profiles C_0 (upwind) and C_1 (downwind) in the right panels, and the implied particle transmission fraction C_1/C_0 in the left panels. Some profiles for Windbreak 2 (runs 13 to 17) are not shown as the trend is the same as for the data presented.

Typically, C_1/C_0 is approximately uniform at values around 0.1 to 0.2 over most of the windbreak height. There is a sharp increase in C_1/C_0 near the top of the windbreak, associated with the decrease in leaf area density there as the windbreak becomes ragged near its top. For some profiles the ratio C_1/C_0 behaves quite erratically, but these are always associated with very low values of the upwind concentration C_0 (so that the denominator in the ratio is small), and hence may be ascribed to measurement errors when the amount of spray arriving at the windbreak is too small.

Height-averaged values of the particle transmission fraction C_1/C_0 were calculated by averaging C_0 and C_1 separately over the lower two thirds of the windbreak height, where C_1/C_0 is approximately uniform, and taking the quotient of the averaged C_1 and C_0. The average C_1/C_0 was 0.112 ± 0.050 (sample standard deviation over 18 runs) for the mass-based fluorometric method, and 0.209 ± 0.080 (sample standard deviation over 12 runs) for the droplet-counting method. (One outlier, arising from low upwind concentrations, was omitted from each of these averages). The average optical porosity t_b across all runs was 0.104 ± 0.011 (sample standard deviation over 23 runs). From these results we conclude that:

- From the mass-based fluorometric measurements, the simple approximation $C_1/C_0 \approx t_b$ (Equation (7)) is supported.

- There is a disagreement between the values of C_1/C_0 from the fluorometric method and from droplet counting. This is attributed to different weightings of the two methods with respect to particle size. Fluorometry gives a measure of concentration weighted by the total mass of droplets intercepted by the target, whereas droplet counting gives a measure weighted by the number of droplets intercepted. Hence the droplet-counting method is biased towards small droplets in the particle size distribution, and the fluorometric method *vice versa*. Since the transmission fraction C_1/C_0 is larger for small particles than large ones, the particle size distribution just downwind of the windbreak will be biased in favour of small particles, relative to the size distribution just upwind. Hence, when size-integrated measures C_1/C_0 are formed, the fluorometric method will give a smaller mean value than the droplet-counting method.

- There is too much run-to-run variability in the data, and insufficient spread in the optical porosities of the experimental windbreaks, to test whether the predicted trend in particle transmission with optical porosity (for instance Equation (7)) is supported by the data. However, it is certainly not contradicted.

Finally, Figure 13 shows the height-averaged values of C_1/C_0 plotted against the reference wind speed, which was measured at height 2 m well upwind of each windbreak. Superimposed on this plot are the predictions of Equation (5) for C_1/C_0, using Equations (17) and (18) to determine

the bleed velocity and Equations (8) and (9) to account for streamlining, calculated at five values of the optical porosity t_b from 0.05 to 0.25 (encompassing the range for the experimental windbreaks, for which t_b was fairly close to 0.1 in all cases), and using other realistic parameter values specified in the figure caption. This plot shows several features:

- There is broad agreement in the predicted and observed trends in C_1/C_0 with wind speed.
- The tendency for C_1/C_0 to increase with wind speed in strong winds is entirely caused by streamlining; it is demonstrated by the predictions and confirmed well by the empirical data.
- At low wind speeds, the data show higher values of C_1/C_0 than the predictions. This may be associated with the fact that the predictions are made for particles of just one diameter (80 μm) whereas the spray in reality has a broad particle size distribution with many droplets much smaller than 80 μm. For these smaller particles, C_1/C_0 is larger at moderate to low wind speeds.

6 Conclusions

The results of this work can be summarised as follows.

Entrapment of particles by the windbreak: A theory for the entrapment of particles in the windbreak itself has been developed and tested against field data. This leads to the following simple guidelines:

- For particles of moderate size (30 μm) and larger, and for all typical vegetation element sizes except very large (over 30 mm), the fraction of particles transmitted through a windbreak is about the same as the optical porosity t_b, and the fraction entrapped by filtration of the airflow is about $(1-t_b)$. For small particles, or for windbreaks with very large leaves, a larger fraction than t_b is transmitted and a smaller fraction than $(1-t_b)$ is entrapped.
- The total number or mass of particles deposited to the windbreak is determined by a trade-off: the windbreak must be dense enough to absorb particles efficiently, but sparse enough to

allow some particles to flow through and be trapped. The value of the optical porosity for maximum total deposition is typically around t_b = 0.2 but depends on several factors.

Attenuation of particle deposition to the surface in the lee of the windbreak: From a simple theory for the attenuation of particle deposition to the surface by local protection in the lee of the windbreak, the following guidelines emerge:

- The protection offered by a windbreak against particle deposition to the downwind surface arises from two effects: entrapment of particles by the windbreak, and wind shelter in the lee of the windbreak.

- Particle entrapment attenuates the deposition immediately behind the windbreak (over a distance of several windbreak heights) by a factor approximately equal to the optical porosity t_b, as above.

- Wind shelter attenuates the deposition in the immediate lee of the windbreak (over several windbreak heights) by about a factor t_b for small particles (around 10 μm and smaller). There is practically no effect of wind shelter on deposition for large particles (over 300 μm).

- Combining both effects, the reduction in deposition in the immediate lee of the windbreak due to both particle entrapment and wind shelter is a factor of about t_b^2 for moderate-sized (30 μm) particles and about t_b for large particles (over 300 μm). For instance, if the optical porosity is 25% = 0.25, then the deposition immediately behind the windbreak is reduced for small particles to about 0.25x0.25 = 0.06 of its upwind value, while for large particles it is reduced to about 0.25 of its upwind value.

- This protection is significant (deposition reduction relative to upwind of over 50%) for a shelter distance of 3 to over 10 windbreak heights downwind. Values at the lower end of this range are appropriate for rough upwind terrain, and at the higher end for smooth terrain. The protection then attenuates gradually with further distance downwind until it disappears at many tens of windbreak heights.

Finally, the outcomes of this consultancy can be reviewed against the four agreed deliverables for the project.

Deliverable 1: Guidelines (in the form of graphs, tables and practical rules of thumb) enabling vegetation management officers and committees to assess the effectiveness of vegetation in providing local or short-range protection for sensitive areas (rivers, pastures, urban areas) against contamination by airborne spray or dust.

This deliverable is met through the above simple rules for use in the field.

Deliverable 2: Scientific justification for these guidelines, derived from models of wind flow and particle deposition to vegetation.

This report, its predecessor (Raupach and Leys 1999) and the ensuing paper (Raupach *et al.* 2001) contain full scientific justification.

Deliverable 3: Results from a wind tunnel study on the aerodynamic (bulk drag) properties of vegetative barriers of different densities.

Results from wind tunnel studies are reported in Figure 8. These were obtained by re-analysis of existing data (Judd *et al.* 1996, Judd *et al.* 2000) rather than by new experiments, since re-analysis was sufficient to provide the information needed for the present study and produced consistent results. We have also provided analysis of field observations which support the main conclusion of the study.

Deliverable 4: A report describing the guidelines and their scientific basis from both modelling and wind tunnel studies.

The present report meets this deliverable.

Acknowledgments: We acknowledge with appreciation the support of the NSW Department of Land and Water Conservation.

References

Chamberlain, A.C. (1967). Transport of *Lycopodium* spores and other small particles to rough surfaces. *Proc. Roy. Soc. London* **A296**, 45-70.

Davidson C.I., and Y.L. Wu. (1990). Dry deposition of particles and vapors. In: *Acidic Precipitation, Vol. 3: Sources, Deposition, and Canopy Interactions* (Eds. S.E. Lindberg, A.L. Page and S.A. Norton). (Springer-Verlag, New York). p. 103-216.

Finnigan, J.J. and Raupach, M.R. (1987). Transfer processes in plant canopies in relation to stomatal characteristics. In: *Stomatal Function* (Eds. E. Zeiger, G.D. Farquhar and I.R. Cowan). (Stanford University Press, Stanford, CA, USA). p. 385-429.

Judd, M.J., Raupach, M.R. and Finnigan, J.J. (1996). A wind tunnel study of turbulent flow around single and multiple windbreaks, Part I: velocity fields. *Boundary-Layer Meteorol*. **80**, 127-165.

Hughes, D.E., Cleugh, H.A., Judd, M.J., Hutchinson, P. and Claessens, E. (2001). Effects of porous windbreaks on airflow and scalar transport I: Wind tunnel experimental design. *Boundary-Layer Meteorol*. (In preparation).

Judd, M.J., Cleugh, H.A. and Hughes, D.E. (2001). Effects of porous windbreaks on airflow and scalar transport II: Wind tunnel results. *Boundary-Layer Meteorol*. (In preparation).

Cleugh, H.A. and Hughes, D.E. (2001). The impact of shelter on crop microclimates: a synthesis of results from wind tunnel and field experiments. *Agroforestry Systems* (In press).

Cleugh, H.A. (2001). Field measurements of windbreak effects on airflow, turbulent exchanges and microclimates. *Agroforestry Systems* (In press).

Monteith, J.L. (1973). *Principles of Environmental Physics*. (Arnold, London).

Raupach, M.R., Finnigan, J.J and Brunet, Y. (1996). Coherent eddies and turbulence in vegetation canopies: the mixing layer analogy. *Boundary-Layer Meteorol*. **78**, 351-382.

Raupach, M.R. and Leys, J.F. (1999). The efficacy of vegetation in limiting spray drift and dust movement. CSIRO Land and Water, Tech. Rep. 47/99.

Raupach, M.R., Briggs, P.R., Ford, P.W., Leys, J.F., Muschal, M. and Cooper, B. (2000a). Endosulfan transport I: Integrative assessment of airborne and waterborne pathways. *Journal of Environmental Quality* (In press).

Raupach, M.R., Briggs, P.R., Ahmad, N. and Edge, V. (2000b). Endosulfan transport II: Modelling airborne dispersal and deposition by spray and vapour. *Journal of Environmental Quality* (In press).

Raupach, M.R., Leys, J.F., Woods, N., Dorr, G. and Cleugh, H.A. (2001). The entrapment of particles by windbreaks. *Atmospheric Environment* (Submitted).

Slinn, W.G.N. (1982). Predictions for particle deposition to vegetative canopies. *Atmos. Environ.* **16**, 1785-1794.

Tables

			Meteorology				Barrier Configuration				
Test	Code	Date	Time	Temp	Dir	U2 (m/s)	H: m	Rows	LAI	Porosity Dem.	Porosity LoneTr
1A	A1	7/03/90			NW-SW	6.5	9.5	1			
1B	A2	7/03/90			NW-SW	11	9.5	1			
1C	A3	12/03/90			E	4.65	9.5	1			
1	T1	17/04/91	7:49	16.9	256	1.5	11	1		0.1	Assum WB2 ir
2	T2	17/04/91					11	1		0.1	
3	T1	18/04/91	7:49	15.2	295	1.5	11	1		0.1	
4	T2	18/04/91	8:32	18.3	295	2	11	1		0.1	
5	T1	29/04/91	8:13	15.5	262	1.6	11	1		0.1	
6	T2	29/04/91	8:44	17.5	262	0.3	11	1		0.1	
7	T3	2/05/91	14:40	28.4	224	2.6	11	1		0.1	
8	T4	2/05/91	14:59	28.2	200	1.6	11	1		0.1	
9	T5	2/05/91	15:27	29.6	227	1.3	11	1		0.1	
10	T6	2/05/91	15:51	28.5	229	1.6	11	1		0.1	
11	T1	16/05/91	9:43	16.2	228	3.1	11	1		0.1	
12	T2	16/05/91	10:08	17	230	2.5	11	1		0.1	
13	T1	30/04/92	9:20	17.9	141 ?	3.1	11	1	2.74	0.11	0.177
14	T2	25/09/92	11:36	27.9	260	5.6	11	1	2.74	0.11	0.177
15	T3	25/09/92	14:11	29.6	266	3.1	11	1	2.74	0.11	0.177
16	T4	30/09/92	12:53	20.1	231	4.2	11	1	2.74	0.11	0.177
17	T5	30/09/92	13:32	21.5	243	4.6	11	1	2.74	0.11	0.177
18	T1	13/10/92	15:52	19.7	133	1.7	9	1	2.85	0.083	0.107
19	T2	13/10/92	16:29	19.1	138	1.1	9	1	2.85	0.083	0.107
20	T3	15/10/92	14:05	23.3	218	3.1	7	2	2.93	0.102	0.073
21	T4	15/10/92	14:37	22.4	1	3.6	7	2	2.93	0.102	0.073
22	T5	15/10/92	17:30	20.2	2	1.8	7	4	4.08	0.132	0.05
23	T6	15/10/92	18:01	19.1	352	0.7	7	4	4.08	0.132	0.05

Table 1: summary of runs in field measurements of particle transmission by windbreaks.

Figures

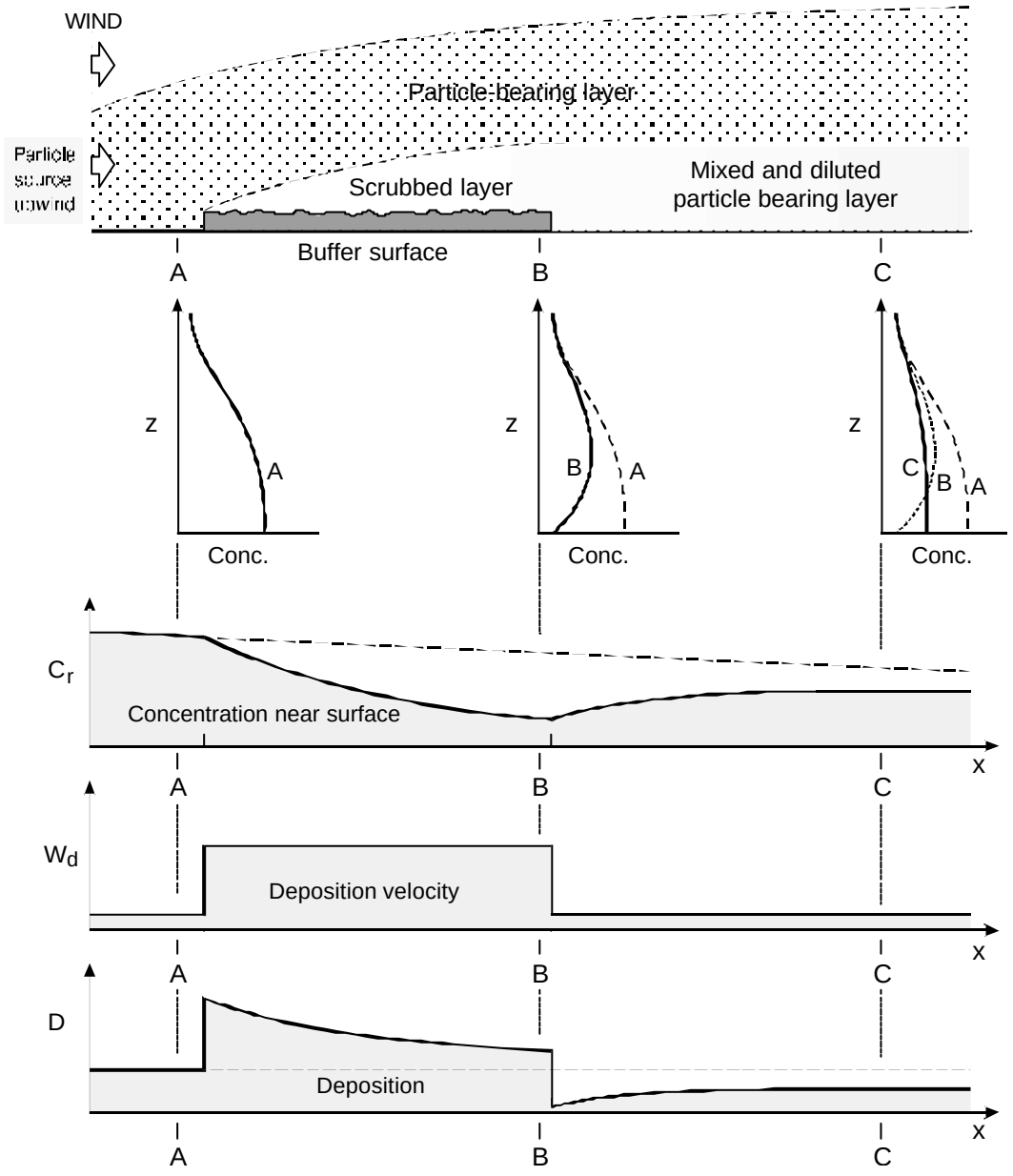

Figure 1: Schematic diagram illustrating mechanism of regional protection against particle deposition to downwind surfaces by a buffer surface with a high potential for particle capture.

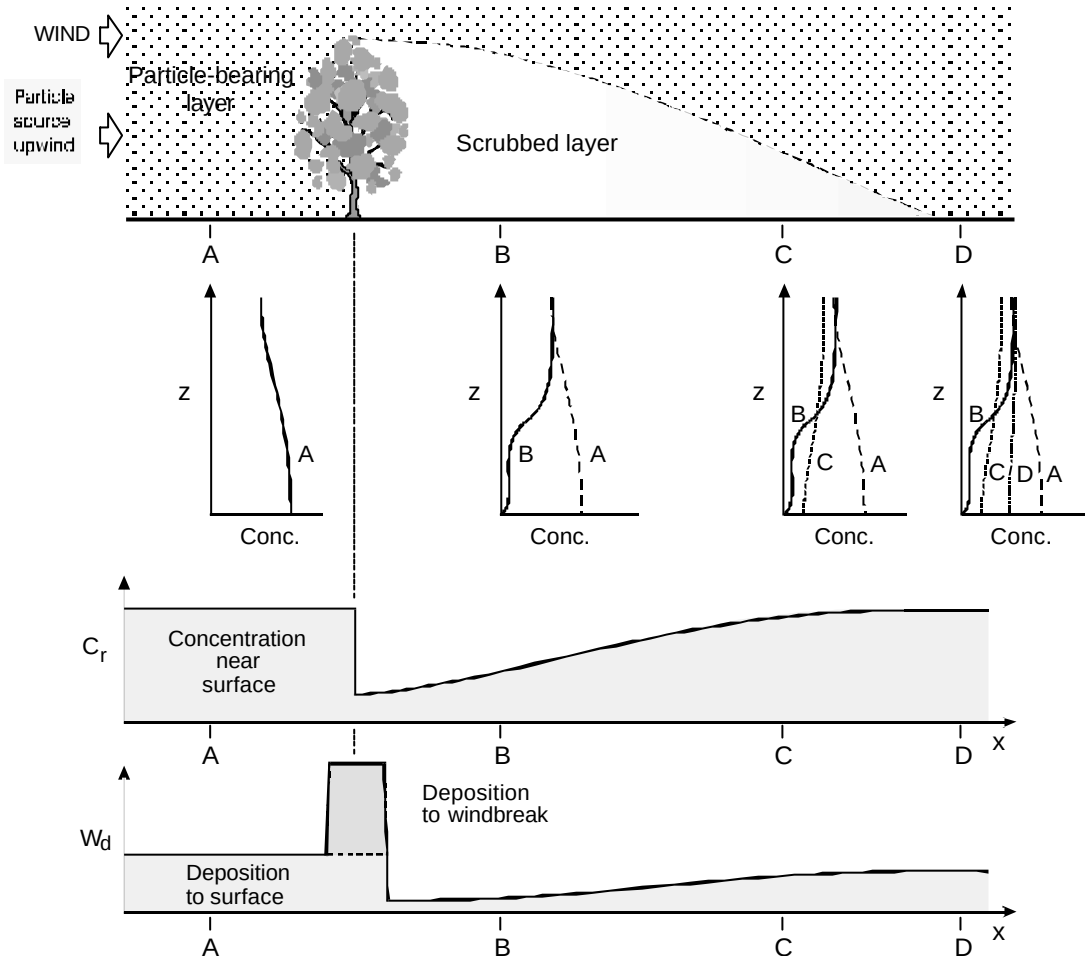

Figure 2: Schematic diagram illustrating mechanism of local protection against particle deposition to downwind surfaces by a porous barrier.

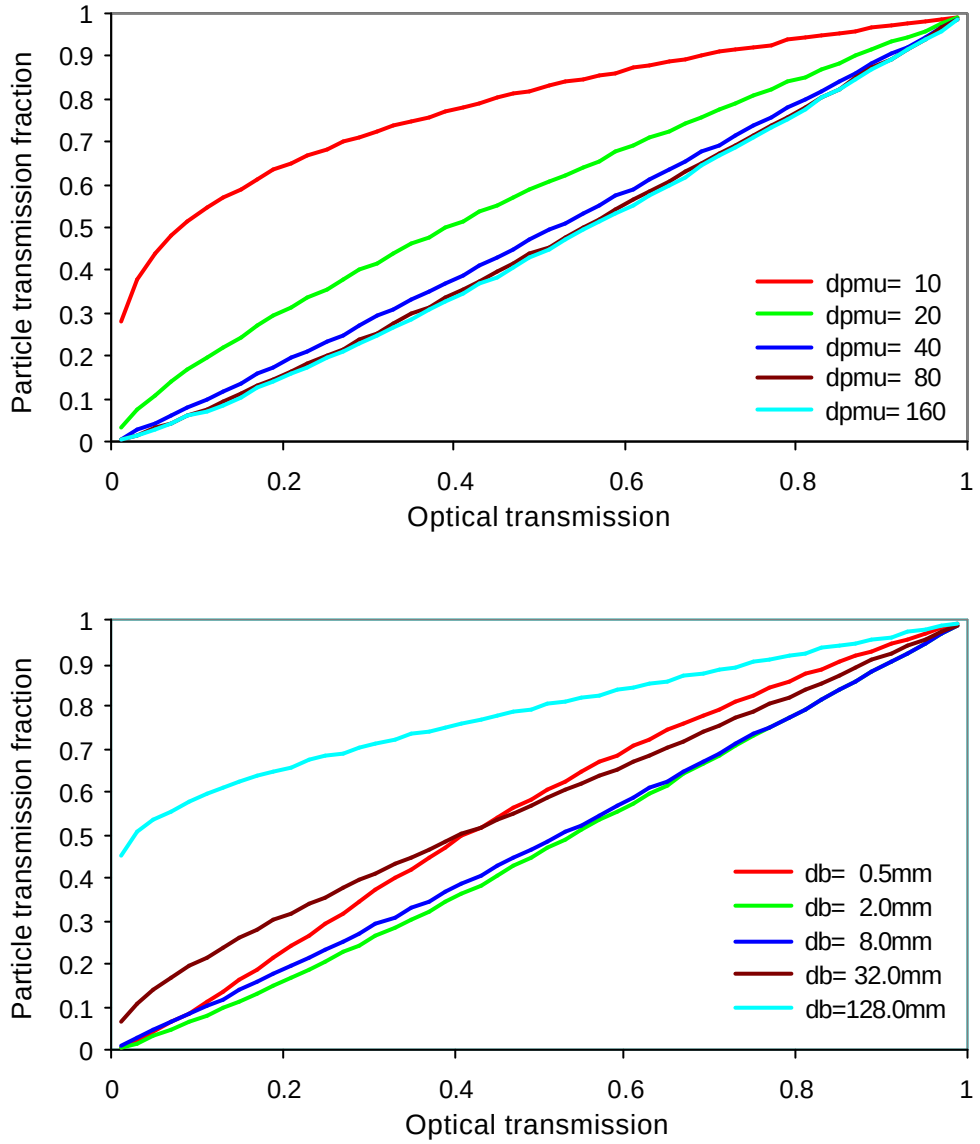

Figure 3: Prediction from Equation (5) for the particle transmission fraction C_1/C_0, plotted against the optical porosity t_b for various particle diameters d_p (upper panel) and various vegetation element diameters d_e (lower panel). Assumed conditions: wind speed through windbreak (U) = 2 m s^{-1}, meander factor (m) = 1.2, d_e = 2 mm (for upper panel), d_p = 80 µm (for lower panel).

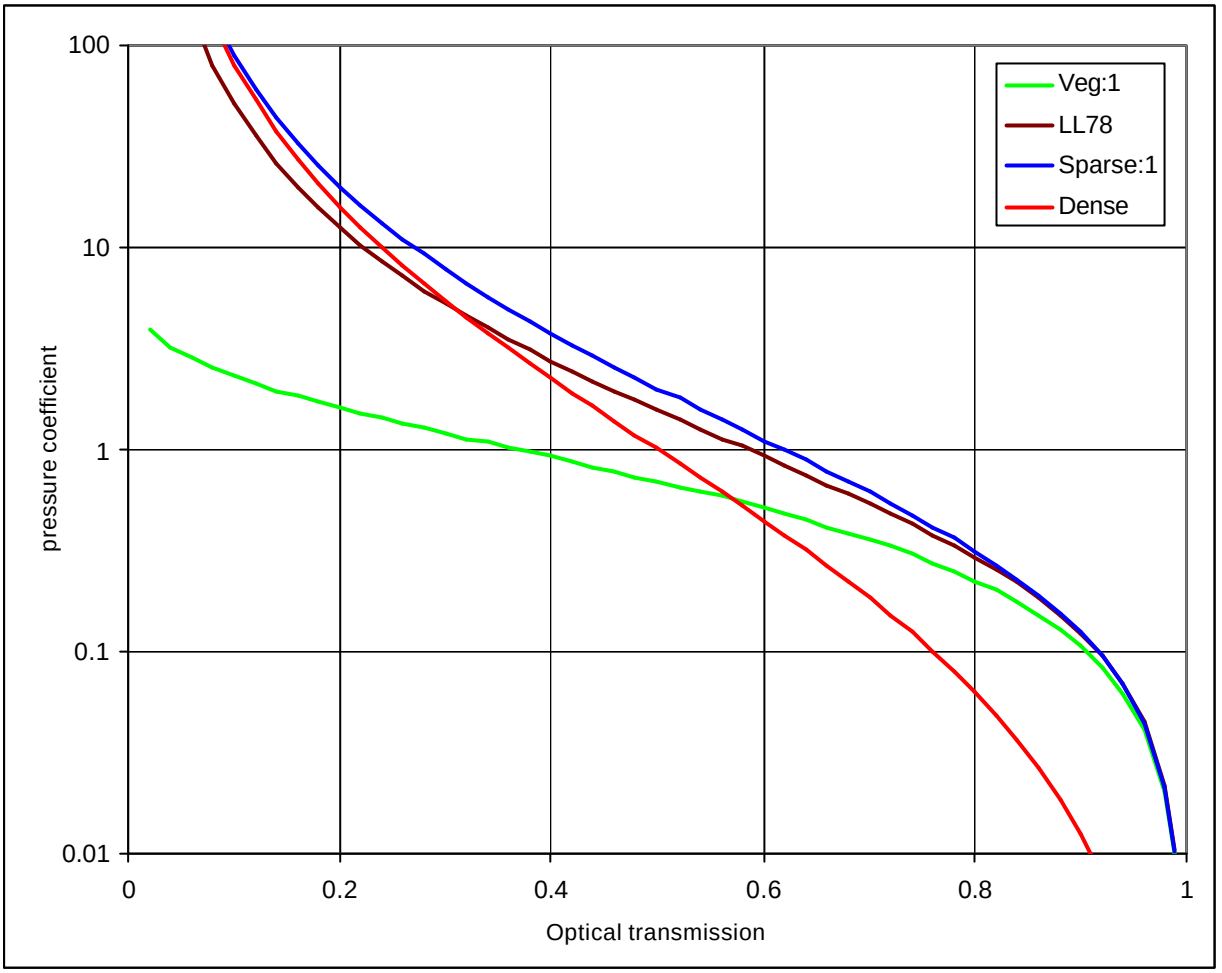

Figure 4: Comparison of formulae for calculating the pressure coefficient k of a screen or vegetative barrier from its optical porosity t_b. Veg: $k = -c_d \ln(t_b)$ (Equation (18)); LL78: Sparse: Dense: Throughout, the element drag coefficient $c_e = 1$. The vegetation formula gives much lower pressure coefficients than all other formulae for t_b less than about 0.6.

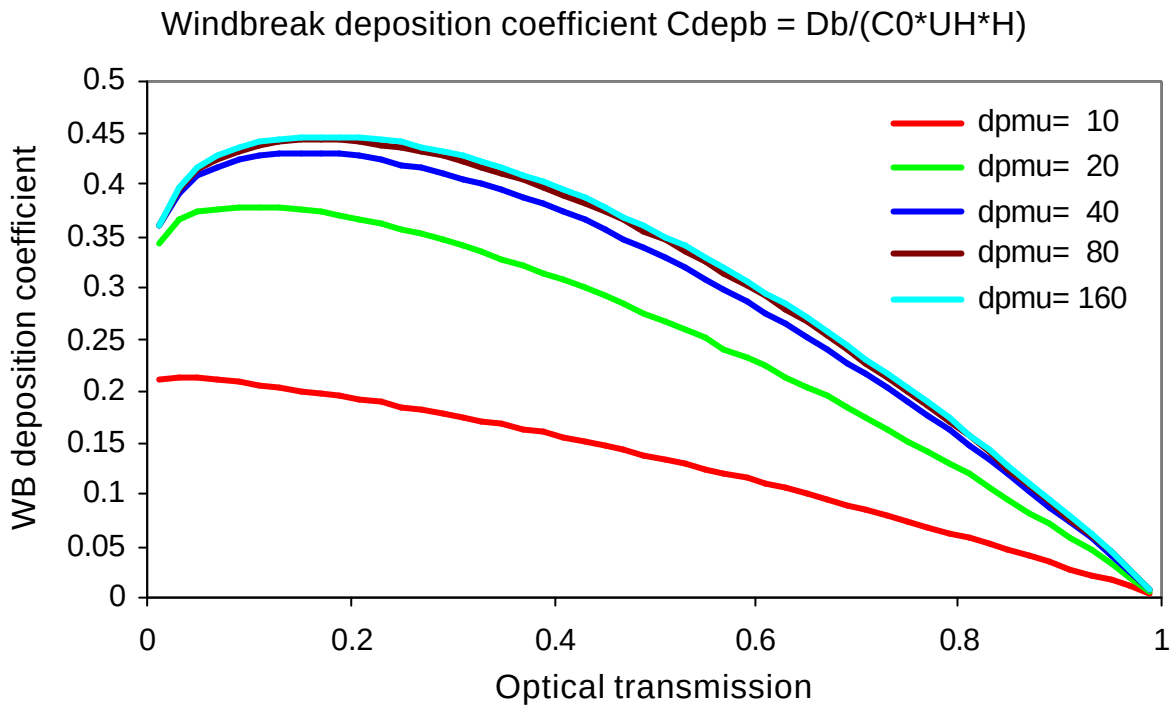

Figure 5: Prediction of Equation (22) for the bulk particle deposition coefficient Δ_b, plotted against t_b for various particle diameters d_p. Assumed conditions: reference wind speed (U_H) = 4 m s^{-1}, meander factor (m) = 1.2, windbreak element diameter (d_e) = 2 mm, windbreak element drag coefficient (c_e) = 1, bulk windbreak drag parameters Γ_{b1} = 0.75, k_1 = 1.5.

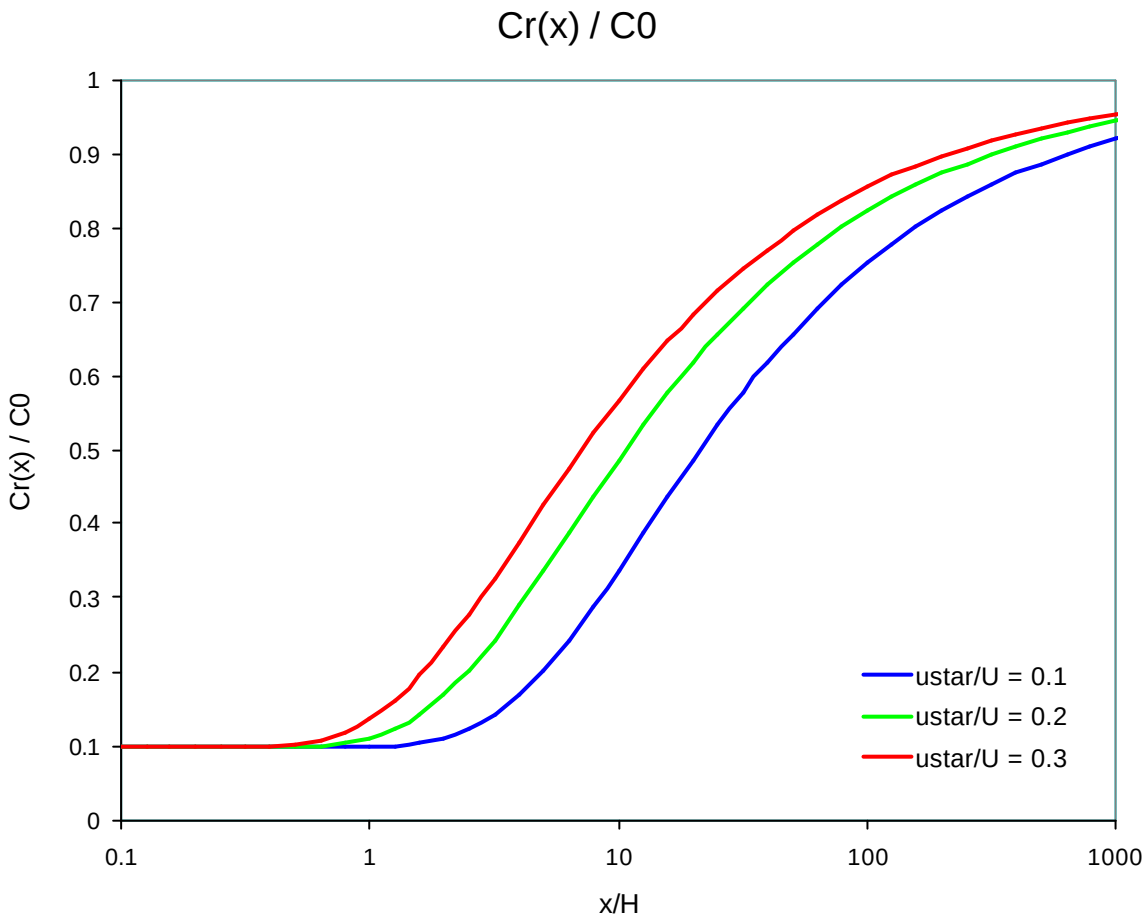

Figure 6: Variation with distance x downwind of the windbreak of the near-surface particle concentration $C_r(x)/C_0$ (normalised with constant upstream concentration C_0), from the solution of the diffusion equation with constant eddy diffusivity and wind speed. It is assumed that $C_1/C_0 = 0.1$, where C_1 is the particle concentration in the filtered air immediately behind the windbreak. The three curves represent different classes of terrain surrounding the windbreak: smooth ($u_*/U = 0.1$), rough ($u_*/U = 0.2$) and very rough ($u_*/U = 0.3$).

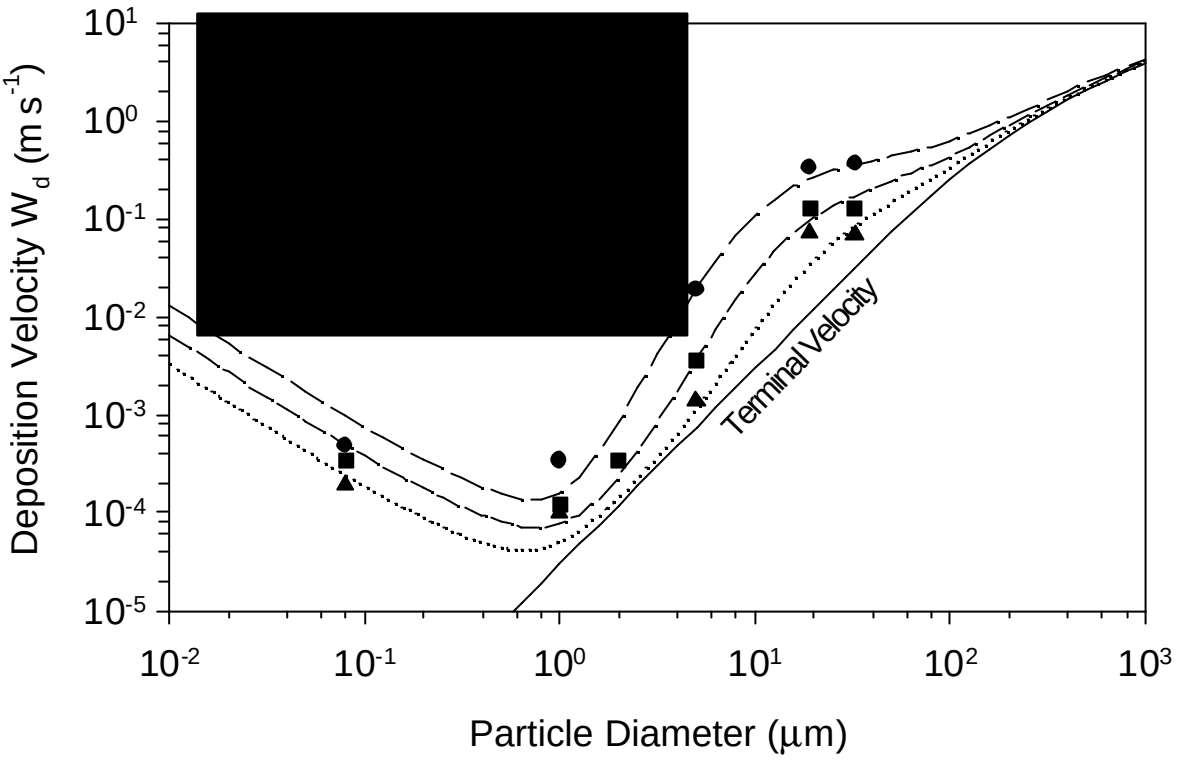

Figure 7a: Test of a single-layer model for the deposition velocity W_d, described in Raupach *et al.* (2000b). Data are wind tunnel measurements of particle deposition to a sticky grass surface by Chamberlain (1967). Predictions are of W_d as a function of particle diameter d_p for vegetation of height 0.06 m and leaf area index 1. Data and predictions are for three wind speeds giving friction velocities (u_*) of 0.35, 0.70 and 1.40 m s^{-1}. The solid line is the predicted terminal velocity W_t as a function of d_p, for spherical particles with the density of water. From Raupach *et al.* (2000b).

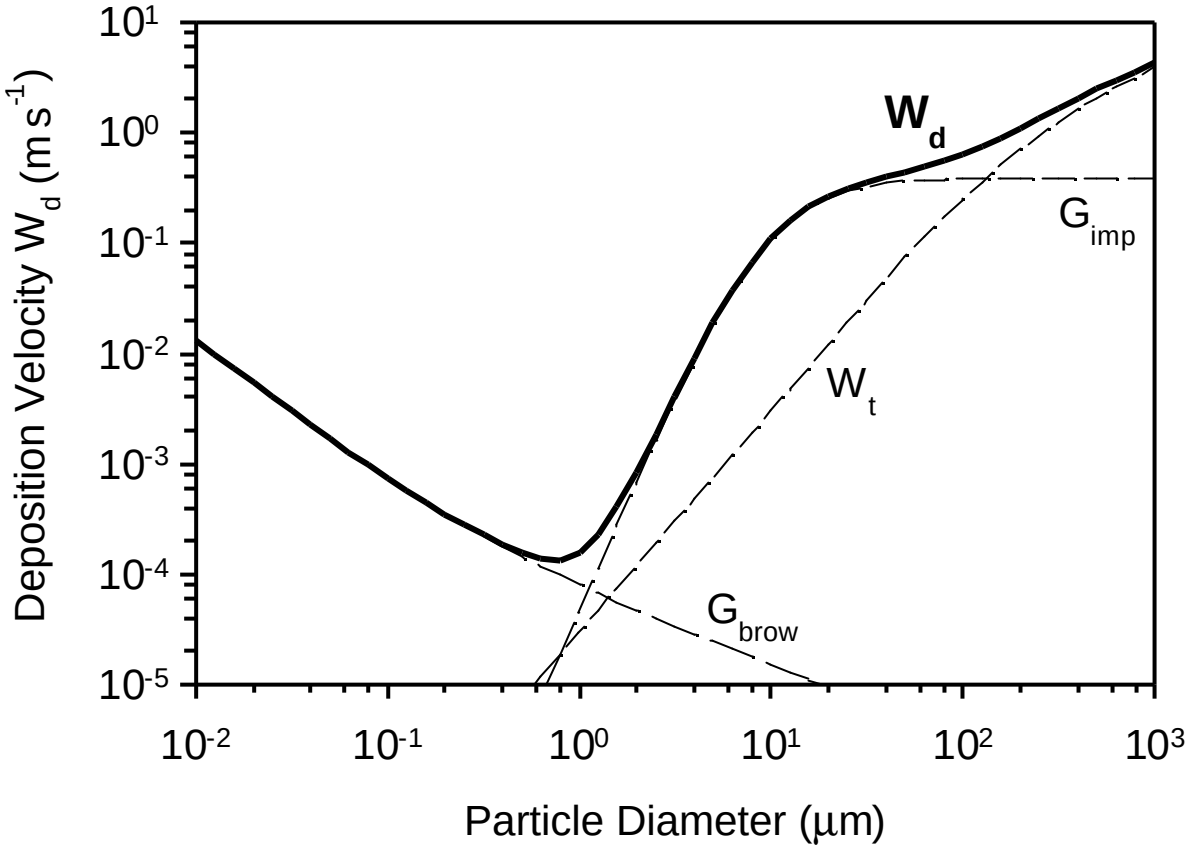

Figure 7b: Contributions of the three terms W_t (settling), G_{imp} (impaction) and G_{brow} (Brownian diffusion) to the deposition velocity W_d. Conditions as in Figure 6 with $u_* = 1.40$ m s^{-1}. From Raupach *et al.* (2000b).

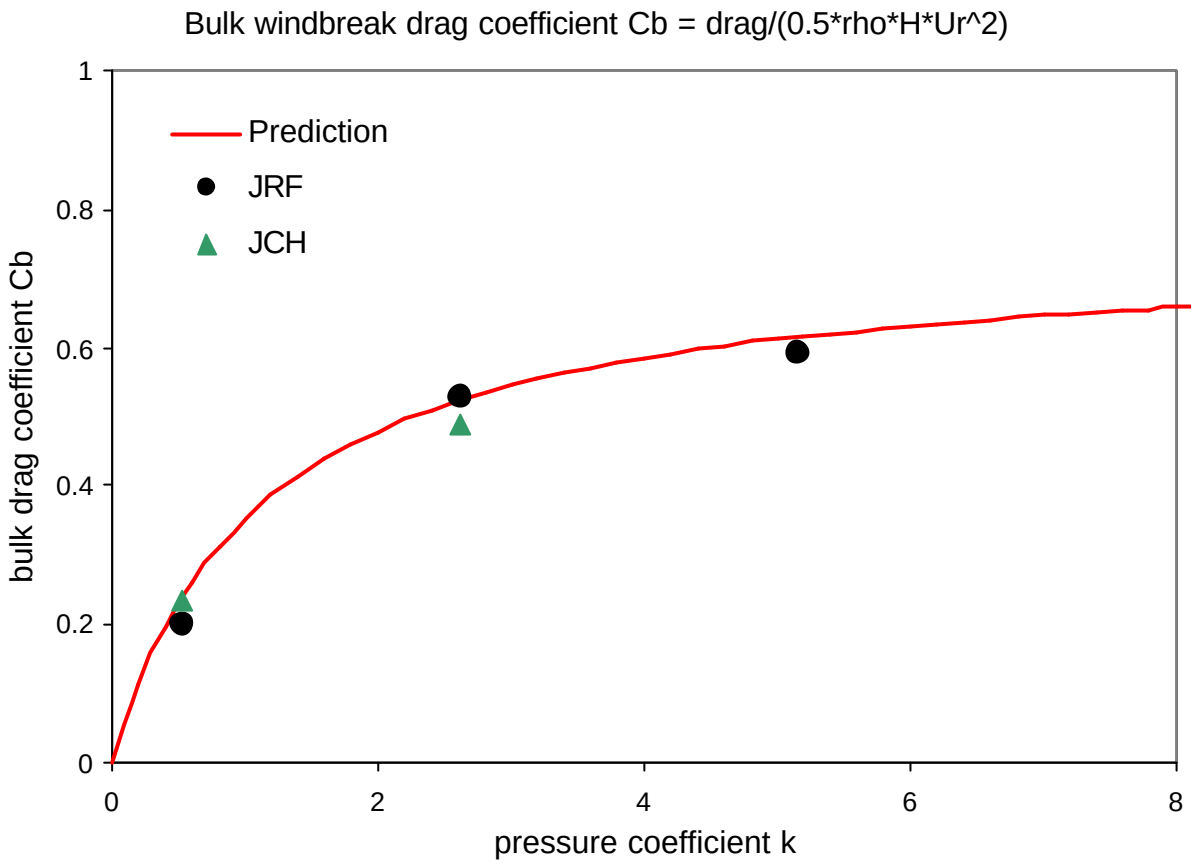

Figure 8: Test of Equation (16) for the bulk drag coefficient of a windbreak, using wind tunnel data from Judd *et al.* (1996, JRF) and Judd *et al.* (2000, JCH). Parameter values: $\Gamma_{b1} = 0.75$, $k_1 = 1.5$.

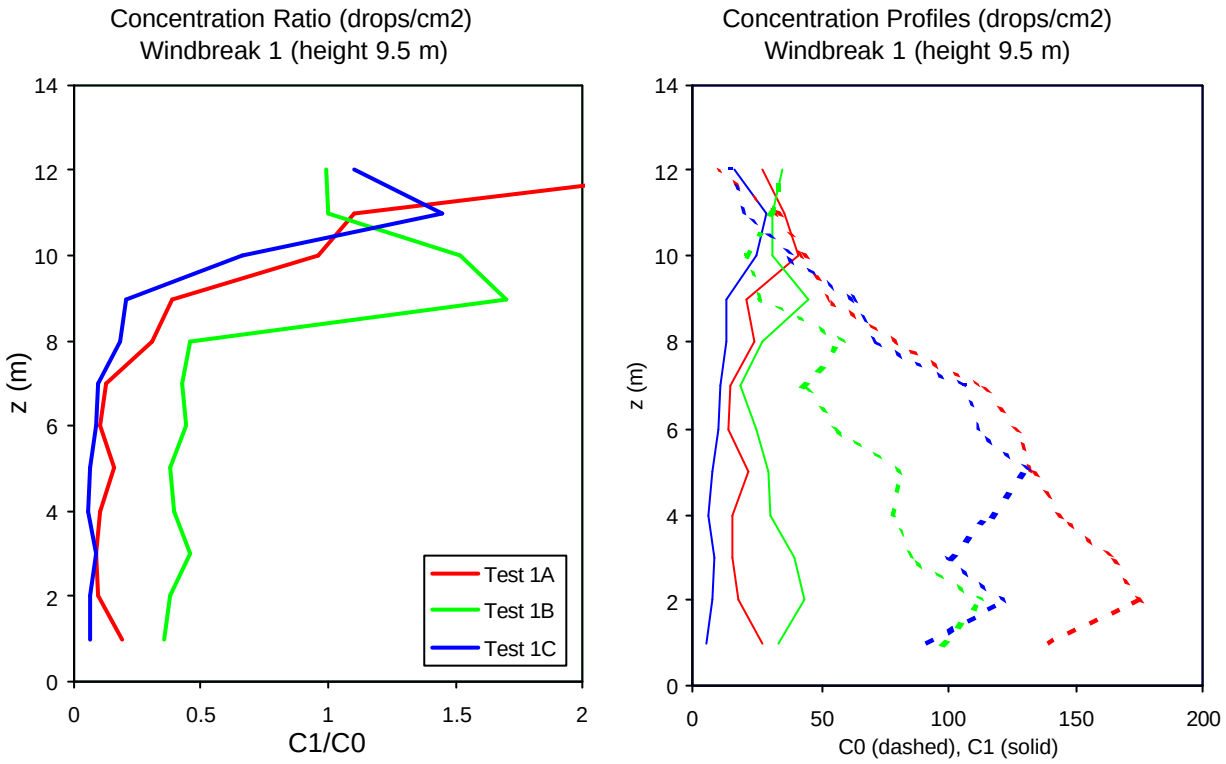

Figure 9: Particle transmission fraction C_1/C_0 (left panel) and concentration profiles C_0 (upwind) and C_1 (downwind) for Windbreak 1. Measurements by droplet recovery.

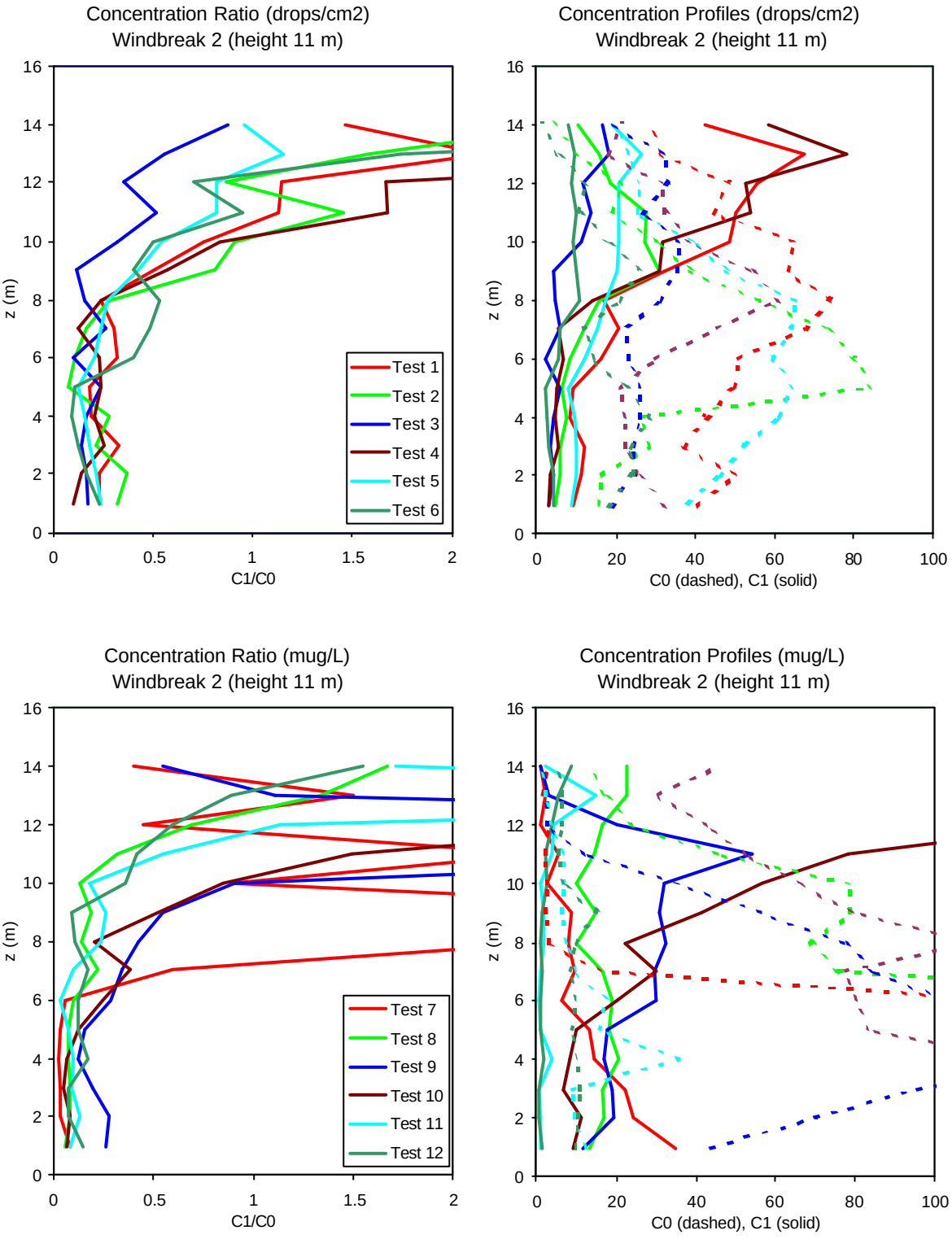

Figure 10: Particle transmission fraction C_1/C_0 (left panel) and concentration profiles C_0 (upwind) and C_1 (downwind) for Windbreak 2. Upper panels: droplet recovery; lower panels: fluorometry.

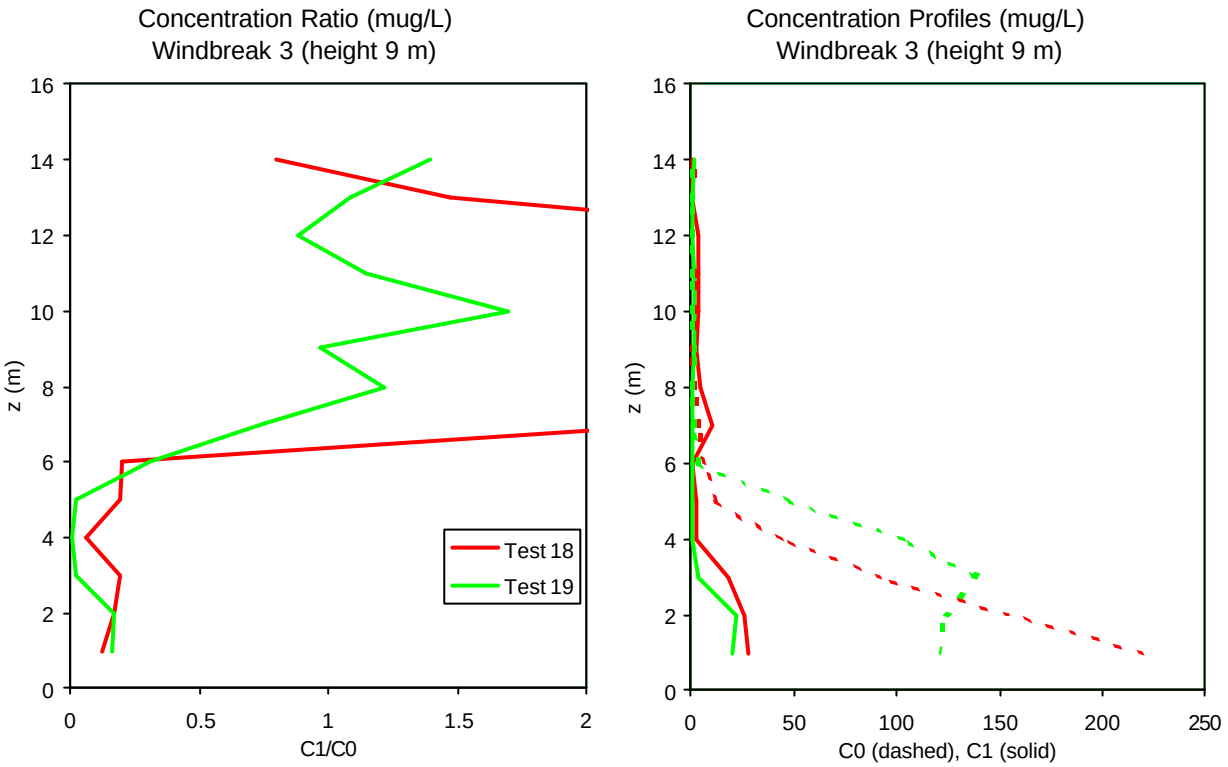

Figure 11: Particle transmission fraction C_1/C_0 (left panel) and concentration profiles C_0 (upwind) and C_1 (downwind) for Windbreak 3. Measurements by fluorometry.

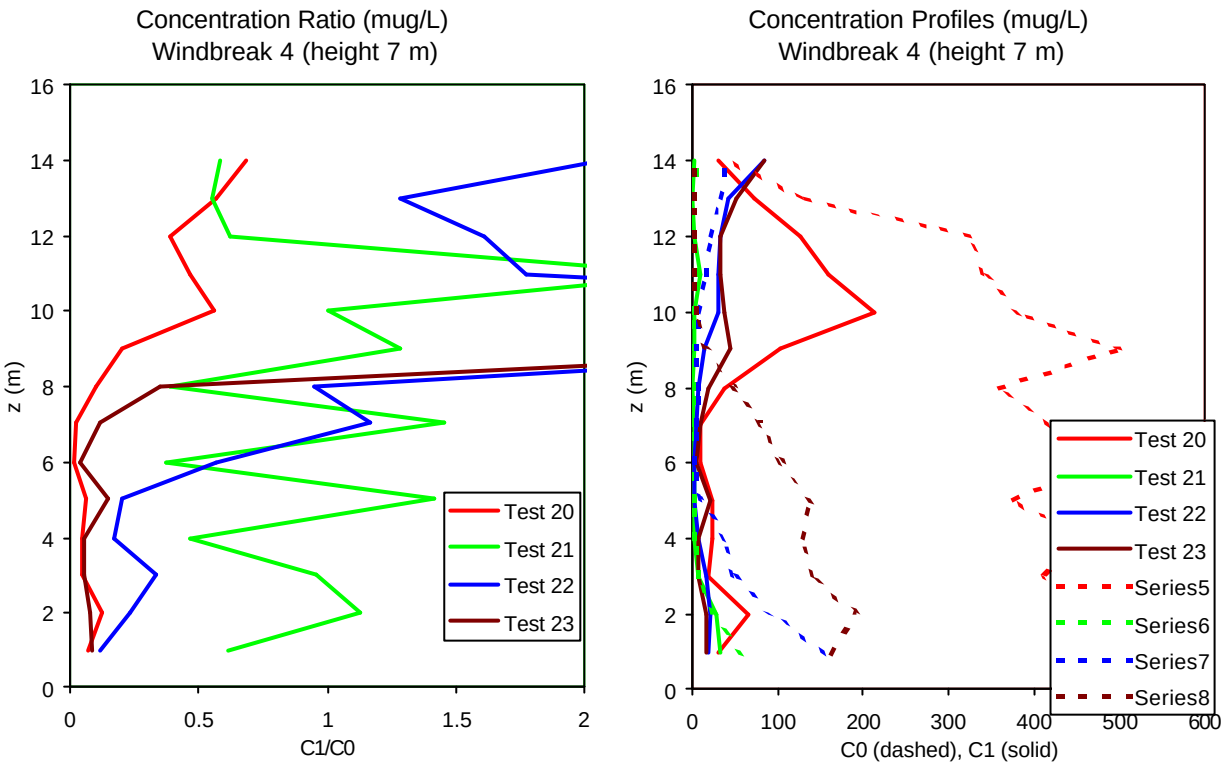

Figure 12: Particle transmission fraction C_1/C_0 (left panel) and concentration profiles C_0 (upwind) and C_1 (downwind) for Windbreaks 4 and 5. Measurements by fluorometry.

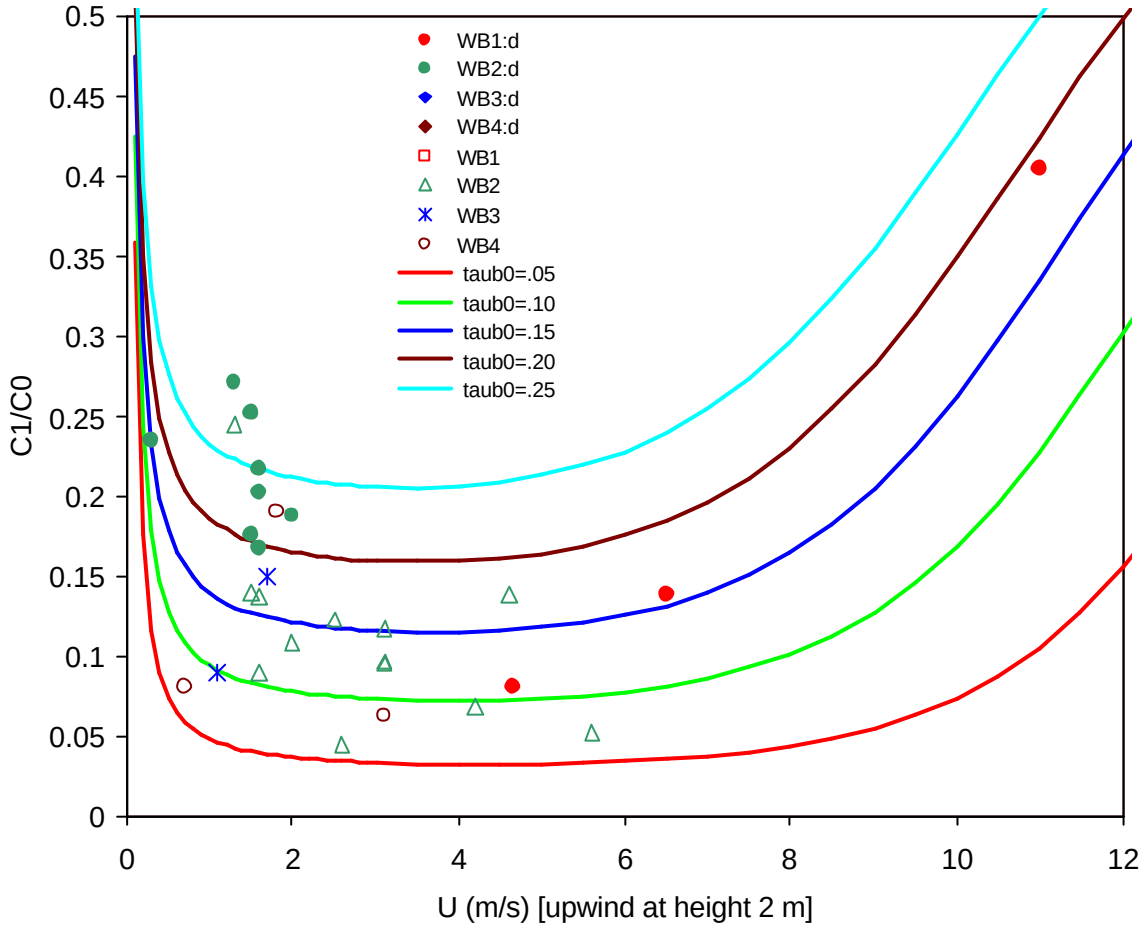

Figure 13: Measured particle transmission fractions C_1/C_0 plotted against reference wind speed (upwind at height 2 m), together with predictions at unstreamlined optical porosities t_{b0} of 0.05, 0.10, 0.15, 0.20 and 0.25. The predictions are based on Equation (5), using Equations (17) and (18) to determine bleed velocity and Equations (8) and (9) to account for streamlining. Assumed conditions: particle diameter d_p = 80 μm, meander factor m = 1.2, windbreak element diameter d_e = 2 mm, windbreak element drag coefficient c_e = 1, bulk windbreak drag parameters Γ_{b1} = 0.75, k_1 = 1.5.